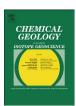


Contents lists available at SciVerse ScienceDirect

Chemical Geology

journal homepage: www.elsevier.com/locate/chemgeo



Contribution of atom-probe tomography to a better understanding of glass alteration mechanisms: Application to a nuclear glass specimen altered 25 years in a granitic environment



S. Gin ^{a,*}, J.V. Ryan ^b, D.K. Schreiber ^b, J. Neeway ^b, M. Cabié ^c

- ^a CEA Marcoule DTCD SECM LCLT, F-30207 Bagnols-sur-Ceze, France
- ^b Pacific Northwest National Laboratory, P.O. Box 999, Richland, WA 99354, USA
- ^c Aix-Marseille Université, CP2M, F-13397 Marseille, France

ARTICLE INFO

Article history: Received 19 December 2012 Received in revised form 28 March 2013 Accepted 1 April 2013 Available online 8 April 2013

Editor: J. Fein

Keywords: Nuclear glass Atom probe tomography Interdiffusion Alteration layers Long-term rate

ABSTRACT

We report and discuss results of atom probe tomography (APT) and energy-filtered transmission electron microscopy (EFTEM) applied to a borosilicate glass sample of nuclear interest altered for 25.75 years at 90 °C in a confined granitic medium in order to better understand the rate-limiting mechanisms under conditions representative of a deep geological repository for vitrified radioactive waste. The APT technique allows the 3D reconstruction of the elemental distribution at the reactive interphase with sub-nanometer precision. Profiles of the B distribution at pristine glass/hydrated glass interface obtained by different techniques are compared to show the challenge of accurate measurements of diffusion profiles at this buried interface on the nanometer length scale. Our results show that 1) Li from the glass and hydrogen from the solution exhibit anti-correlated 15 nm wide gradients located between the pristine glass and the hydrated glass layer, and 2) boron exhibits an unexpectedly sharp profile (~3 nm width) located just outside of the Li/H interdiffusion layer; this sharp profile is more consistent with a dissolution front than a diffusion-controlled release of boron. The resulting apparent diffusion coefficients derived from the Li and H profiles are $D_{Li} = 1.5 \times 10^{-22} \text{ m}^2 \cdot \text{s}^{-1}$ and $D_H = 6.8 \times 10^{-23} \text{ m}^2 \cdot \text{s}^{-1}$. These values are around two orders of magnitude lower than those observed at the very beginning of the alteration process, which suggests that interdiffusion is slowed at high reaction progress by local conditions that could be related to the porous structure of the interphase. As a result, the accessibility of water to the pristine glass could be the rate-limiting step in these conditions. More generally, these findings strongly support the importance of interdiffusion coupled with hydrolysis reactions of the silicate network on the long-term dissolution rate, contrary to what has been suggested by recent interfacial dissolution-precipitation models for silicate minerals.

© 2013 Elsevier B.V. All rights reserved.

1. Introduction

In two previous papers we focused on a long duration experiment involving a monolith of inactive nuclear glass leached at 90 °C in a simulated granitic environment, as it was thought that a comprehensive study of this 25.75 year old sample could help better understand the rate-limiting mechanisms of glass alteration (Gin et al., 2011; Guittonneau et al., 2011). According to recent papers, the question of the rate limiting mechanism in relation with modeling the long term behavior of silicate minerals or glasses in natural environments remains topical and challenging. This is especially true for predicting the fate of $\rm CO_2$ or radionuclides in the perspective of geological disposal of radioactive wastes (Grambow, 2006; Hellmann et al., 2012; Gin et al., 2013). Various techniques such

E-mail addresses: stephane.gin@cea.fr (S. Gin), joe.ryan@pnnl.gov (J.V. Ryan), daniel.schreiber@pnnl.gov (D.K. Schreiber), james.neeway@pnnl.gov (J. Neeway), martiane.cabie@univ-amu.fr (M. Cabié).

as scanning electron microscopy (SEM), transmission electron microscopy (TEM). Raman microspectroscopy and NanoSIMS applied to this altered glass sample provided detailed information about the structure, porosity and chemical composition of the alteration layers. In particular, it was shown that the altered regions of the glass (~7 µm total thickness) in the upper part of the glass block consisted of three distinct layers: i) an internal 'hydrated glass' layer adjacent to the pristine glass, so named because of its structural similarity to that of the glassy silicate network and its simultaneous enrichment in water and select elements supplied by the solution (K), ii) an intermediate 'gel layer' that exhibited large pores and a reorganized silicate network and iii) an outer layer of crystalline phases that precipitated during leaching (mainly phyllosilicates). Compared to short-term experiments conducted in conditions representative of a potential geological disposal environment $(T < 100 \, ^{\circ}\text{C}, 6 < \text{pH} < 10)$, the hydrated glass layer was thicker by orders of magnitude, allowing for the first time to delve into it with detailed microscopy. In particular, steep chemical gradients were apparent, especially for B, which is considered a tracer species of the glass dissolution reaction. The location, shape, and thickness of such a gradient can be tied to the

^{*} Corresponding author. Tel.: +33 466791465.

protective properties of the alteration layer. Indeed, on the basis of only a few direct observations, it was assumed that alteration layers are protective when saturation conditions are achieved, i.e. when the concentration of silica, which is the main glass former, has reached a steady state concentration in solution. Such a protective effect is supposedly achieved by the limitation of transport of water molecules and water-soluble species released by the glass through the alteration layers. However, the processes remain insufficiently understood. Accurate characterization of the chemical gradients within the alteration layers would thus provide significant insight into their protective properties, and thus allow improvements on the existing models (Hellmann et al., 2012).

In our previous paper we observed an apparent gradient of B of 170 nm thickness using NanoSIMS working with a Cs⁺ primary beam, focused to a spot size to ~80 nm which precluded the quantification of the B gradient to any better resolution (Gin et al., 2011). To overcome this limitation, two other complementary analytical techniques capable of higher spatial resolution have been pursued: energy-filtered transmission electron (EFTEM) and atom probe tomography (APT). This paper reports the resulting findings from these high-resolution techniques and discusses their implication in terms of rate limiting mechanisms in glass dissolution at high reaction progress.

2. Materials and methods

2.1. Glass

This study was conducted on SON68 glass, the inactive surrogate of the French R7T7 glass produced at La Hague, where spent nuclear fuel in France is reprocessed and the waste vitrified. Its composition is shown in Table 1 for the major elements and in Guittonneau et al (2011) for the whole composition.

2.2. Alteration experiment

This section aims to describe only the primary features of the long-term alteration experiment. For more details refer to Guittonneau et al. (2011). A cylindrical SON68 glass block 70 mm in diameter and 80 mm high was leached for 25.75 years in slowly renewed "granitic groundwater" (at 90 °C, 100 bar) in contact with sand and some pieces of granite and steel as repository environmental materials (Fig. 1a and b). The leaching solution was a commercial mineral water, called *Volvic*; its composition has changed little during the test. The main constituents of this solution are: Si (23.0–31.7 mg·L $^{-1}$), Ca (9.8–11.5 mg·L $^{-1}$), Na (9.2–11.6 mg·L $^{-1}$), Mg (5.4–8.0 mg·L $^{-1}$), K (5.5–6.2 mg·L $^{-1}$), Cl (7.0–13.5 mg·L $^{-1}$), SO $_4^2$ (7.2–8.1 mg·L $^{-1}$), HCO $_3$ (65.9–71 mg·L $^{-1}$), and NO $_3$ (1.0–6.3 mg·L $^{-1}$) and the pH ranged between 7.0 and 7.2. During the test, 163 solution samples were used to calculate from the B

Table 1Nominal and APT-measured concentrations of various species in both pristine glass and hydrated glass (in at.%). Indicated error is the standard deviation of the measured concentration from 2 pristine glass samples and 4 hydrated layer samples.

	Nominal	APT – pristine	APT — hydrated
Al	2.01	2.51 ± 0.08	2.17 ± 0.12
В	8.41	6.38 ± 0.01	1.63 ± 0.08
			< 0.5 estimated
B (elemental signal only)	N/A	1.06 ± 0.09	0.06 ± 0.01
Ca	1.50	1.9 ± 0.03	2.44 ± 0.15
Fe	0.76	1.54 ± 0.15	1.6 ± 0.11
Н	0.00	2.65 ± 0.32	11.45 ± 1.51
K	0.00	0.2 ± 0.02	0.45 ± 0.15
Li	2.77	2.5 ± 0.23	0.16 ± 0.14
Mo	0.25	0.69 ± 0.02	0.68 ± 0.10
Na	6.64	4.86 ± 0.59	0.45 ± 0.21
0	59.13	52.16 ± 0.08	52.86 ± 1.08
Si	15.81	18.92 ± 0.09	20.69 ± 0.86
Zr	0.45	1.16 ± 0.07	1.16 ± 0.07

release the mean altered glass thickness ($28 \pm 9 \,\mu m$) and the glass dissolution rate. For the last 24 years, the mean alteration rate remained very constant at $6 \times 10^{-3} \, \mathrm{g \cdot m^{-2} \cdot d^{-1}}$, about 20 times higher than the residual rate (i.e. the minimum and virtually constant rate reached once the solution is saturated with respect to silicon) as measured in a batch reactor at the same temperature and about 200 times lower than the initial rate (Gin et al., 2012).

At the end of the experiment, SEM analyses were performed on many specimens sampled from the entire glass block. In the upper half, the general morphology of the alteration layer consisted of a relatively uniform gel and some crystalline phases, which were rare-earth phosphates and clay minerals; the mean measured thickness of this alteration layer was 7 μ m, i.e. 4 times lower than the mean value reported for the whole block. In the lower half of the glass block, however, the alteration layer was thicker. It has been shown that these differences were likely due to chemical gradients in the solution resulting from low hydrodynamic transport of aqueous species.

2.3. Glass sample selected for APT and TEM characterizations

Of the many specimens obtained from the glass monolith, most of the investigations have been carried out on a sample taken in the upper part as the alteration layers were more homogeneous in this part of the block and the corresponding mean alteration rate was closer to the residual rate measured in static conditions. For this study we have selected areas very close to those characterized in our previous study (Gin et al., 2011). Fig. 1c shows the alteration layers probed by APT. It consists of a 1 μm thick internal layer (hydrated glass), a 7.5- μm thick gel layer and a fewhundreds-of-nm thick outer layer of crystalline phases. The total volume of the alteration layers for the entire block is very close to the glass volume loss predicted by the amount of boron in solution (Guittonneau et al., 2011). Extrapolating this result to a local scale, we calculate a mean alteration rate at the location studied of $2.2 \times 10^{-3}~{\rm g\cdot m^{-2} \cdot d^{-1}}$ (i.e. $9.3 \times 10^{-15}~{\rm m\cdot s^{-1}}$). This last value is obtained by dividing the rate, expressed in ${\rm g\cdot m^{-2} \cdot d^{-1}}$, by the glass density (2.75 ${\rm g\cdot cm^{-3}}$) and converting the result into SI units.

2.4. Atom probe tomography

2.4.1. Sample preparation

Specimens for APT analysis were extracted from a polished cross-section of the corroded piece using standard FIB lift-out procedures for APT specimens with a dual-beam SEM/FIB (FEI Helios Nanolab 600) (Thompson et al., 2007). Specimens were sharpened into the necessary conical APT specimen geometry using annular mill patterns with 30 kV $\rm Ga^+$ FIB and final specimen cleanup to minimize ion-beam damage was performed with 2 kV $\rm Ga^+$ FIB. The final tip diameter was ~100 nm.

2.4.2. Analyses by atom probe tomography

Atom-probe tomography (APT) is an analytical technique that combines three-dimensional, sub-nm spatial resolution with single-atom sensitivity of all elements independent of atomic number. While the technique has focused traditionally on electrically-conductive metallic specimens, the technique can also be applied to non-conductive specimens through laser-assisted field ionization. APT analyses were performed with a Cameca LEAP 4000XHR in laser pulsing mode ($\lambda = 355$ nm) (Gault et al., 2012; Kelly and Larson, 2012). The laser pulse repetition rate was set between 100 and 200 kHz, the laser pulse energy between 50 and 120 pJ/pulse, and the target evaporation rate between 0.002 and 0.005 detected ions per pulse. The indicated range of analysis parameters did not result in any significant differences in measured composition or spatial resolution for pristine or hydrated SON68 glass. APT reconstruction parameters were estimated based on the analysis volume measured by SEM imaging of each specimen prior to and after APT analysis. The estimated evaporation field for pristine SON68 glass

Download English Version:

https://daneshyari.com/en/article/4698954

Download Persian Version:

https://daneshyari.com/article/4698954

<u>Daneshyari.com</u>